

Dalton Transactions

Accepted Manuscript



This is an *Accepted Manuscript*, which has been through the Royal Society of Chemistry peer review process and has been accepted for publication.

Accepted Manuscripts are published online shortly after acceptance, before technical editing, formatting and proof reading. Using this free service, authors can make their results available to the community, in citable form, before we publish the edited article. We will replace this *Accepted Manuscript* with the edited and formatted *Advance Article* as soon as it is available.

You can find more information about *Accepted Manuscripts* in the [Information for Authors](#).

Please note that technical editing may introduce minor changes to the text and/or graphics, which may alter content. The journal's standard [Terms & Conditions](#) and the [Ethical guidelines](#) still apply. In no event shall the Royal Society of Chemistry be held responsible for any errors or omissions in this *Accepted Manuscript* or any consequences arising from the use of any information it contains.



www.rsc.org/dalton

Cite this: DOI: 10.1039/c0xx00000x

www.rsc.org/xxxxxx

ARTICLE TYPE

The Effect of Central and Planar Chirality on the Electrochemical and Chiral Sensing Properties of Ferrocenyl Urea H-Bonding Receptors

Andrea Mulas,^a Yasmine Willener,^a James Carr-Smith,^a Kevin M. Joly,^b Louise Male,^a Christopher J. Moody,^b Sarah L. Horswell*^a Huy N. Nguyen and James H. R. Tucker*^a

Received (in XXX, XXX) Xth XXXXXXXXX 20XX, Accepted Xth XXXXXXXXX 20XX

DOI: 10.1039/b000000x

A new series of chiral ureas containing one or two redox-active ferrocene units was synthesised and studied in order to investigate the effect of planar chirality and central chirality on electrochemical chiral sensing. Binding of chiral carboxylate anions in organic solvents through H-bond formation caused a negative shift in the potentials of the ferrocene/ferrocenium (Fc/Fc⁺) couples of the receptors, demonstrating their use as electrochemical sensors in solution. While the presence of two ferrocene units gave no marked improvement in the chiral sensing capabilities of these systems, the introduction of planar chirality, in addition to central chirality, switched the enantiomeric binding preference of the system and also caused an interesting change in the appearance of some voltammograms, with unusual two-wave behaviour observed upon binding a protected proline guest.

Introduction

The separation of enantiomers and the quantification of enantiomeric excess, for example in the screening of asymmetric reactions, are important processes in chemistry. Supramolecular approaches to these challenges generally involve the design of functional receptors that allow the chiral composition of analytes to be read out in a convenient manner, with the majority of these designed so that binding triggers an optical sensing response.¹ At the same time, it is well established that electrochemistry offers a powerful means for monitoring supramolecular binding events through the use of redox-active tags such as ferrocene.^{2,3} Electrochemical sensors can show high sensitivity and immediacy in the readout and suitable receptors can also be immobilised onto electrode surfaces⁴ to give devices with enhanced sensing properties. However, despite the ubiquitous use of ferrocene moieties for supramolecular sensing purposes, still only a few examples of redox-active receptors designed for chiral sensing are known in the literature.^{5,6,7}

Previous studies in our group focused on the electrochemical sensing of chiral organic molecules using simple enantiopure receptors containing a centrally chiral stereogenic centre located between the binding site and the redox-active ferrocene unit.^{6,7} In these studies, the supramolecular interaction to bind the guest consisted of either H-bond formation involving a urea group⁶ or the formation of a reversible covalent boronate ester adduct,⁷ with the latter giving the better results in terms of electrochemical chiral sensing. In the meantime, however, we also reported the convenient synthesis of ferrocenyl urea derivatives bearing both planar chirality and central chirality.⁸ Given these findings and the fact that ferrocene derivatives of this type can act as convenient organometallic asymmetric catalysts,⁹ we decided to probe the effect on electrochemical chiral sensing of introducing

planar chirality into urea-based H-bonding receptors. Therefore, building on the previous studies on receptor **1** with three chiral carboxylate anions,^{6b} a new series of receptors **2-6** (Figure 1) were accordingly synthesised and their interactions with these same guests **7-9** (Figure 2) probed by various spectroscopic and voltammetric techniques, as described herein. The binding studies demonstrate how subtle differences in structure can affect not only the capacity for electrochemical chiral sensing but also the type of voltammetric behaviour observed.

Results and Discussion

Synthesis

The synthesis of receptor **1** was reported previously and was made *via* a reaction between the corresponding ferrocenyl amine and *p*-nitrophenylisocyanate.^{6b} This involves the use of a chiral auxiliary to generate the precursor to the amine with high diastereoselectivity (*ca.* 95% de). The synthesis of **2**, containing both planar chirality and central chirality, followed a similar route. In this case, the same chiral amine used previously to generate the analogous thiourea⁸ was used. A diastomeric ratio (dr) of *ca.* 95:5 was determined by ¹H NMR analysis of the urea prior to purification. In our previous work,⁸ we had established that planar chirality overrode the stereocontrol caused by the chiral auxiliary used to determine the diastereoselectivity in the insertion of the chiral group on the receptor.⁸ For this reason, only some combinations of the two elements of asymmetry could be obtained for this study. The enantiomeric pair (*R*_p)-**3** and (*S*_p)-**3** containing planar chirality alone, were made *via* a known asymmetric synthesis procedure^{8,10,11} to generate ferrocene aldehydes. The aldehydes were then converted to the

corresponding amines (Scheme 1), which in turn were then reacted with *p*-nitrophenylisocyanate to afford the targets (*R_p*)-**3** and (*S_p*)-**3** in good enantiomeric excess, as calculated by analysis of chiral HPLC traces. The previously reported achiral urea **4**¹² was synthesised in a similar fashion *via* the known ferrocenyl methylamine **13**¹³ using literature procedures.^{14,15} The synthesis of the bis-ferrocenyl receptor **5** was achieved *via* the same chiral ferrocenylamine (**12**) used for the synthesis of **1**,^{6b} which in this case was reacted with 1,1'-carbonyl diimidazole¹⁶ in anhydrous DMF to give the desired product (Scheme 2). The achiral analogue **6** was synthesised in a similar manner using amine **13**, noting that it already been prepared by Molina *et al.* *via* a different route.^{3f}

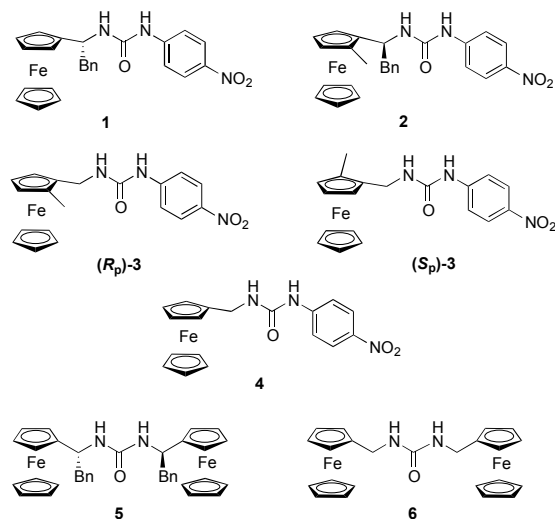


Fig. 1 Previously studied receptor **1** and novel receptors **2-6**.

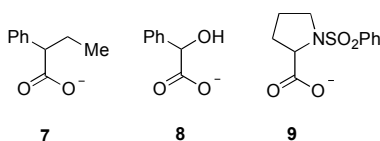
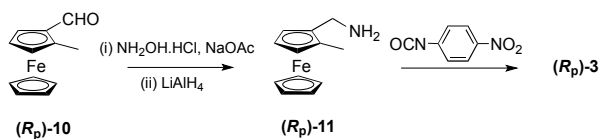
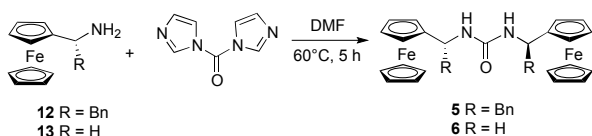


Fig. 2 Chiral carboxylates used as guests (as tetrabutylammonium salts).



Scheme 1 Synthetic route to the planar chiral ureas **3**, shown for (*R_p*)-**3**



Scheme 2 Synthetic route to the bis-ferrocenyl ureas **5** and **6**

X-Ray crystal structures

Crystals of five receptors were found to be suitable for X-Ray diffraction experiments. Those of the mono-ferrocenyl receptors (*R_p*)-**3**·0.5 H₂O and (*S_p*)-**3**·0.5 H₂O were obtained by slow evaporation of a solution in deuterated chloroform and those of **4** were produced by slow evaporation of a solution in a mixture of CH₂Cl₂ and Et₂O. Crystals of **5**·H₂O and **6** were formed from slow evaporation of a solution in Et₂O. The structure of **5**·H₂O is presented in Figure 3 and the other structures are included in the supporting information.

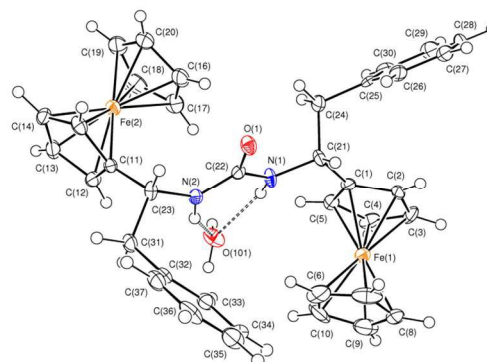


Fig. 3 Crystal structure of the chiral receptor **5**·H₂O with ellipsoids drawn at 50% probability level. Dotted lines correspond to H-bonding. A water molecule is included in the crystal. All hydrogen atoms are reported.

The structure of **5**·H₂O has the expected (*R*) configuration of the α -carbon atoms ((*R_p*)-**3**·0.5 H₂O and (*S_p*)-**3**·0.5 H₂O also show the expected stereochemistry) and also depicts the urea binding site inside a pseudo-cavity created by the ferrocenyl and the benzyl groups. The size and flexibility of this cavity determines guest binding strength as well as selectivity (*vide infra*). The binding site is occupied by one water molecule, which is interacting with the urea NH groups through two hydrogen bonds.

Binding Studies: NMR and UV-vis spectroscopy

¹H NMR binding studies in organic solvents using the tetrabutylammonium (TBA) salts of carboxylates **7-9** were performed on the receptors to assess the binding mode and stoichiometry of the complexes. Representative Job plots (5 mM) showed the expected 1:1 host/guest stoichiometry, as found in examples previously reported for compound **1**.^{6b}

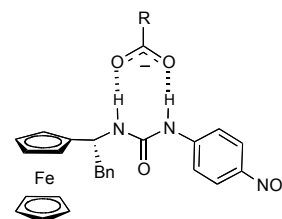


Fig. 4 Depiction of the H-bonding interaction between carboxylate anions and the ferrocenyl receptors in this study (shown for receptor **1**).

In all cases, the signals for the NH protons in the urea groups shifted downfield upon addition of the guests, which confirmed the expected urea-carboxylate interaction, consisting of two H-bonds (Fig. 4). As also found previously for **1**,^{6b} the binding of the guests **7-9** by receptors **1-4** in common organic solvents was too strong for accurate binding constant values to be determined at NMR concentrations. However for receptors **5** and **6**, the situation was different, presumably because of the more hindered cavity created by the presence of two ferrocene units, as well as the absence of the electron withdrawing nitrobenzene moiety which would be expected to increase H-bonding strength. Therefore, ¹H NMR titrations to quantify the binding interactions were performed for these two receptors, in CD₃CN for **5** but in 2:1 CD₃CN/CD₂Cl₂ for **6** for solubility reasons. The resulting data in the form of stacked ¹H NMR spectra are reported in the supporting information. For the achiral receptor **6**, the same NH shift value was obtained for a given aliquot of either enantiomer. However, for the chiral receptor **5**, after the addition of 5 molar equivalents, the shift reached was *ca* 7.2 ppm for (*R*)-**9** and *ca* 7.5 ppm for (*S*)-**9**, indicating different binding characteristics for the two diastereomeric complexes. The data obtained from the titrations were fitted to a 1:1 binding model using the software WinEQNMR.¹⁷ The resulting binding constant values were the same for the achiral receptor (120 M⁻¹ for **6**:(*S*)-**9** and 121 M⁻¹ for **6**:(*R*)-**9**) but sufficiently different (error < 6%) for the chiral receptor to indicate at best modest enantioselectivity: 258 M⁻¹ for **5**:(*S*)-**9** and 217 M⁻¹ for **5**:(*R*)-**9**.

As found previously for **1**,^{6b} a bathochromic shift in the nitrobenzene chromophore (λ_{\max} *ca* 350 nm) present in receptors **2-4** allowed calculation of the binding constants by UV-Vis spectroscopy. However in order to calculate accurately the values *via* the chosen Benesi-Hildebrand method,¹⁸ it was necessary to perform the UV-Vis titration experiments in DMSO. In this competitive solvent, a sufficiently large excess amount of guest has to be added before an appreciable amount of complex is formed, which satisfies the Benesi-Hildebrand conditions. Representative data are given in the supplementary information and the resulting binding constants for receptors **2-4** are presented in Table 1, together with the values previously obtained for receptor **1**.^{6b} Different values and shifts in the absorption band for the different guests **7-9** were observed. In general, guest **8** was bound the most weakly and **7** the most strongly, in line with the trend observed previously.^{6b} This may arise at least in part from differences in the *pK_a* values of the conjugate acids of the guests, which is lower for mandelic acid than for the other guests, making **8** the weakest H-bonding base.

Table 1 Binding constant values for the five hosts with both enantiomers of the three guests, expressed as log*K* (\pm 0.05) in dry DMSO (host 0.025 mM and guest 6.25 mM) at rt. Obtained with UV-Vis spectroscopy using the Benesi-Hildebrand method.

| | (<i>S</i>)- 7 | (<i>R</i>)- 7 | (<i>S</i>)- 8 | (<i>R</i>)- 8 | (<i>S</i>)- 9 | (<i>R</i>)- 9 |
|------------------------------------|------------------------|------------------------|------------------------|------------------------|------------------------|------------------------|
| 1 ^a | 3.42 | 3.33 | 2.98 | 2.93 | 3.25 | 3.03 |
| 2 | 3.38 | 3.39 | 2.47 | 2.52 | 3.06 | 2.82 |
| (<i>R_p</i>)- 3 | 3.37 | 3.37 | 2.53 | 2.56 | 2.93 | 2.93 |
| (<i>S_p</i>)- 3 | 3.36 | 3.35 | 2.54 | 2.52 | 2.93 | 2.93 |
| 4 | 3.23 | 3.24 | 2.58 | 2.59 | 2.96 | 2.98 |

^aData from reference 6b.

As expected, the experiments in DMSO with the achiral receptor **4** gave the same binding constants for either enantiomer of the same guest, within experimental error (\pm 0.05). However, the only host/guest combination in which any degree of chiral recognition was observed (*i.e.* outside of experimental error) was for receptors **1** and **2** towards guest **9**. It is likely that this arises from a combination of π -stacking interactions and increased steric effects with this guest. However, it is particularly interesting to note that receptor **2** is slightly selective towards the same (*S*) guest as receptor **1**, despite possessing the opposite central chirality. Consequently, it appears that planar chirality plays an important role in directing the selectivity of the receptor. However, the experiments with the enantiomeric pair of receptors (*R_p*)-**3** and (*S_p*)-**3**, which contain only planar chirality, indicate no chiral selectivity towards enantiomers of the three chiral guests under investigation (Table 1). Therefore, the data indicate that planar chirality alone does not relay chiral discrimination properties to these receptors in the same way that central chirality does in the case of the binding of **1** by guest **9**. However, rather like our previous findings in the synthesis of these systems,⁸ planar chirality can direct the stereochemical preference (*i.e.* its presence results in favourable binding of the *S* enantiomer over the *R* enantiomer being retained) when used in combination with central chirality.

Binding Studies: Electrochemistry

Electrochemical experiments were next performed in order to investigate the redox and sensing behaviour of the hosts and their complexes. First the half-wave potentials, $E_{1/2(\text{H})}$, *vs* dmfc (decamethylferrocene, internal reference) of receptors **1-6** in MeCN were measured using square wave voltammetry, with these reported in Table 2.

Table 2 Half-wave potentials, $E_{1/2(\text{H})}$, (mV \pm 2 mV) *vs* dmfc of the receptors **1-7** (*ca* 3×10^{-4} M in dry MeCN with 0.1 M TBAPF₆ at rt.)

| | 1 ^a | 2 | (<i>R_p</i>)- 3 | (<i>S_p</i>)- 3 | 4 | 5 | 6 |
|---------------|-----------------------|----------|------------------------------------|------------------------------------|----------|----------|----------|
| $E_{1/2}$ /mV | 523 | 473 | 470 | 470 | 517 | 495 | 503 |

^aData from reference 6b. $E_{1/2}$ of dmfc is -0.507 V *vs.* ferrocene in CH₃CN and TBAPF₆ (see ESI for more details).

As expected, the potentials for the mono-ferrocenyl receptors were found to be less positive for receptors **2**, (*R_p*)-**3** and (*S_p*)-**3**, than for **1** and **4**, because the presence of the electron donating methyl substituent on one of the cyclopentadienyl rings increases the electron density on the iron centre and stabilises the higher oxidation state.¹⁹ The potentials of the bis-ferrocenyl receptors were more negative than those for **1** and **4**, because of the absence of the electron withdrawing nitrobenzene group.

The reversibility of each redox process was assessed using cyclic voltammetry. In each case, the intensity of the cathodic peak current was found to be similar to that of the anodic peak.²⁰ In addition, the CVs of the hosts displayed a linear relationship between i_p and the square root of the scan rate, in accordance with the Randles-Sevcik equation.²¹ The peak separations, $E_{\text{pa}} - E_{\text{pc}}$, were *ca* 80 mV, which is consistent with a one-electron process, given that the slightly wide peak separation (*i.e.*, > 59 mV) is likely to be a result of uncompensated Ohmic drop. The bis-

ferrocenyl receptors **5** and **6** gave one single redox wave, which is best explained by there being two superimposed single electron transfer processes. The two peripheral ferrocene moieties of the molecules are therefore independent and do not communicate with each other.²²

Titration experiments involving consecutive additions of carboxylate guests to a solution of each receptor in dry MeCN (concentration *ca* 0.5 mM) were then performed using square wave voltammetry. Each experiment resulted in negative shifts in the observed potentials, indicating the successful electrochemical sensing of these guests. After addition of up to five equivalents of guest (up to 20 equivalents for receptors **5** and **6** because of weaker binding), no more changes were observed, giving in each case a value for the redox potential of the complex, $E_{1/2(\text{HG})}$. Values for the redox response to complexation, ΔE , where $\Delta E = E_{1/2(\text{HG})} - E_{1/2(\text{H})}$, are displayed in Table 3. The same shifts were recorded using CV, but SWV data were preferred where possible, owing to the smaller errors in recording the data. As found previously,^{6b} the size of the negative shift was found to depend on the guest. The generally smaller shifts for **8** can be explained by the lower basicity of this guest, as already discussed above.

For almost all of the complexes studied, the voltammograms exhibited “one-wave behaviour” during the titrations. In other words, the wave for the free receptor gradually shifted to more negative potentials upon the addition of increasing amounts of the guest species (e.g. Fig 6a). However a notable degree of “two-wave behaviour” was observed for complexes between receptor **2** and prolinatate guest **9**. As shown in Fig. 6b, this is signified by the original redox wave at the free host potential decreasing while another emerges at the complexed receptor potential, albeit with some merging of the two waves. The effect was observed using either cyclic or square-wave voltammetry but was more noticeable with the latter. Such behaviour has been noted and discussed previously,^{23,3c} with two-wave behaviour favoured for more strongly binding complexes.^{23a} This explanation would account for the differences observed between guests **8** and **9** for receptor **2** (**9** forms the stronger complex, Table 1) but not for the absence of any substantial two-wave behaviour for the even more strongly bound complexes between these guests and receptor **1**.^{6b} Other factors, such as the magnitude of ΔE and the change in diffusion coefficient upon complexation, which could affect both the appearance and resolution of the redox waves, are discussed in more detail in the supplementary information.

The data in Table 3 indicate that the final shifts observed for all the complexes are the same for each enantiomer of guests **7-9**, in that any differences in ΔE fall within the confidence limit of each experiment. However in our previous studies, when this was found to be the case for receptor **1**, we then demonstrated that by plotting ΔE_{obs} vs equivalents of either enantiomer of guest **9**, the resulting binding curve could be used to indicate a degree of electrochemical chiral sensing for this system.^{6b} However, in the case of the new chiral receptors **2**, (*R_p*)-**3**, (*S_p*)-**3** and **4** studied here, the enantioselectivities were not sufficiently different to indicate effective chiral sensing (see ESI).

The system for receptor **2** with guests (*S*)- and (*R*)-**9** was next examined in more detail, which gave a difference in the enantiomeric sensing response that in fact was only just within the confidence limit (± 4 mV) of the experiments. In fact,

repeated experiments indicated that the full shift was always larger upon addition of guest (*S*)-**9** than (*R*)-**9**. However, the two-wave behaviour meant that it was not possible to plot a titration of ΔE_{obs} vs molar equivalents of guest added. Instead the intensity of current at a chosen potential vs the equivalents of guest added was plotted (Fig. 7). The intensity values were normalised against the peak intensity of the host in its free form, in order to be able to compare the current intensity at a given potential after addition of either enantiomer of the guest. The potential 340 mV vs. dmfc was chosen in order to maximise the difference in the variation of current intensity between the different enantiomers (dashed line in Figure 7a). Values of the current intensity were then plotted as a function of molar equivalents of guest in Figure 7b. Notwithstanding the noted confidence limits in ΔE for this particular system, these studies indicate that monitoring the current change at a fixed potential appears to be an effective method for comparing the redox sensing response of two guest species, in particular for those systems that give a two-wave voltammetric response.

Table 3 Shifts (in mV) in the potential, ΔE , obtained from SWV experiments of the receptors upon addition of an excess amount of guests **8-10** as TBA⁺ salts, in dry MeCN with 0.1 M TBAPF₆ at rt (confidence limit ± 4 mV).

| | (<i>S</i>)-7 | (<i>R</i>)-7 | (<i>S</i>)-8 | (<i>R</i>)-8 | (<i>S</i>)-9 | (<i>R</i>)-9 |
|------------------------------------|------------------|------------------|------------------|------------------|------------------|------------------|
| 1 | -81 ^a | -82 ^a | -59 ^a | -63 ^a | -83 ^a | -78 ^a |
| 2 | -89 ^a | -91 ^a | -74 ^a | -68 ^a | -91 | -84 |
| (<i>R_p</i>)- 3 | -75 | -78 | -60 | -63 | -76 | -73 |
| (<i>S_p</i>)- 3 | -79 | -77 | -63 | -61 | -76 | -74 |
| 4 | -73 | -74 | -59 | -58 | -72 | -73 |
| 5 | nd | nd | nd | nd | -76 | -73 |
| 6 | nd | nd | nd | nd | -85 | -87 |

^a from CV experiments (± 10 mV). Data for **1** taken from reference 6b.

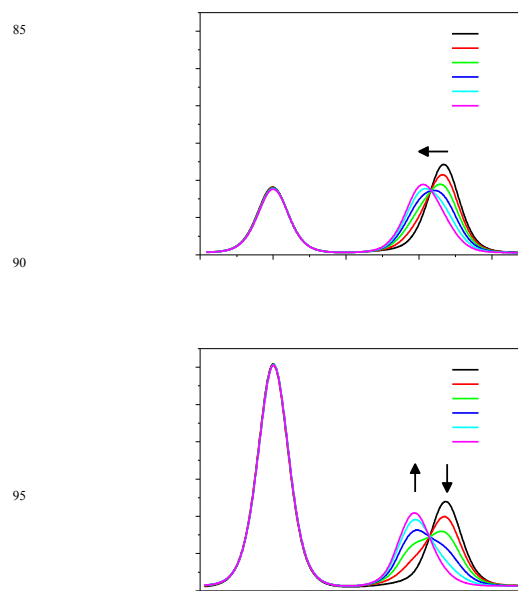


Fig. 6 Differences in electrochemical behaviour for **2** upon addition of (a) guest (*S*)-**8** (one-wave behaviour) and (b) guest (*S*)-**9** (two-wave behaviour). Voltammograms referenced to internal reference dmfc at 0 V.

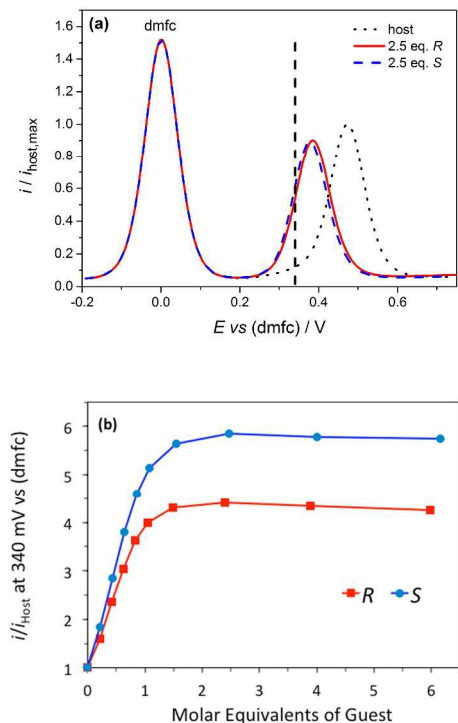


Fig. 7 (a) SWVs of **2** and **2+9**; the dashed line indicates the potential where i/i_{host} is taken. (b) Values of i/i_{host} at 340 mV vs dmfc against molar equivalents of guest added for **2** upon addition of **9**. (Host conc. 0.5 mM, TBAPF₆ 0.1 M, in MeCN at rt). Current values are normalised against the peak intensity of the free host.

Conclusions

A new series of chiral ureas containing two redox-active ferrocene groups, or one ferrocene group and the chromophore *p*-nitrobenzene, has been successfully synthesised and studied. Binding of chiral carboxylate anions through H-bonding causes a negative shift in the ferrocene potentials, which indicates that these receptors can be used to electrochemically sense organic anions in solution at millimolar concentrations. While the introduction of planar chirality alone does not improve the enantioselectivity of these systems, it can modify the properties of the receptor system by not only affecting its enantioselective preference but also unusually changing its voltammetric characteristics, which can switch from one-wave to two-wave behaviour. While these supramolecular systems can clearly respond electrochemically to binding events, further structural improvements to generate better enantioselectivities and more distinct electrochemical signals would be required to deliver more effective chiral sensing.

Experimental Section

The data, conditions and parameters used for the X-ray crystallography, electrochemistry and digital simulations are

described in the ESI.

Synthesis. Compounds **1**^{6b} and **4**^{12,19} and (*R*_p/*S*_p)-**9**^{10,11} were prepared as described previously. Identical procedures to those reported previously^{6b,8} were used to synthesise new compounds **2**, (*R*_p)-**3** and (*S*_p)-**3** from the corresponding amines. Commercially available solvents and reagents were used without further purification, except THF, MeCN and CH₂Cl₂, which were dried in Pure Solv™ Solvent Purification Systems, and DMSO, which was distilled from CaH₂ and kept under argon and in the presence of activated molecular sieves.²⁹ All reactions were carried out under an argon atmosphere with the exclusion of moisture. Thin layer chromatography plates were visualised under UV light or by potassium permanganate stain. Flash chromatography was carried out using silica 60, with the eluent specified. Elemental analysis was determined with a CE Instruments EA1110 elemental analyser. ¹H NMR spectra were recorded at 300 MHz with a Bruker AVIII300 NMR spectrometer, ¹³C NMR spectra at 100 MHz with a Bruker AVIII400 NMR spectrometer, at room temperature. Chemical shifts (δ) are reported in ppm and coupling constants (J) are reported in Hz. MS were recorded with a Waters/Micromass spectrometer using the ES+ method. Optical rotations were measured with a digital polarimeter. The enantiomeric excess of the receptors was calculated from the area of the peaks obtained in the chiral HPLC, performed using an AD column and a 10% iso-propanol (IPA) in hexane mixture of eluents with a flow rate of 1 mL/min, monitoring at 210 nm.

(*S*,*R*_p)-(-)-*N*-[1-(1- α -(Methyl)ferrocenyl-2-phenyl)ethyl]-*N*'-4-nitrophenylurea **2**. 4-Nitrophenyl isocyanate (30 mg, 0.183 mmol) was reacted with (*S*,*R*_p)-(-)-1-[α -(Methyl)ferrocenyl]-2-phenyl-1-ethylamine⁸ (45 mg, 0.141 mmol) and purified by column chromatography on silica gel (EtOAc/light petroleum 1:4) to give the product (63 mg, 92%) as an orange oil. $[\alpha]_{\text{D}}^{25} = -40$ ($c = 0.76$ in acetone); ¹H NMR (400 MHz, (CD₃)₂CO) $\delta = 9.11$ (s, 1H, *NHAr*), 8.46 - 8.57 (m, 2H, *ArH*), 8.08 - 8.19 (m, 2H, *ArH*), 7.45 - 7.65 (m, 3H, *ArH*), 7.28 - 7.41 (m, 2H, *ArH*), 6.66 - 6.77 (m, 1H, *CHNH*), 5.36 - 5.50 (m, 1H, *CHNH*), 4.28 - 4.54 (m, 8H, *CpH*), 3.32 - 3.41 (m, 1H, *ArCHH*), 3.11 - 3.22 (m, 1H, *ArCHH*), 2.05 (s, 3H, *CpCH₃*); ¹³C NMR (101 MHz, CDCl₃) $\delta = 153.6$ (C, CO), 145.7 (C, *Ar*), 142.1 (C, *Ar*), 137.1 (C, *Ar*), 130.0 (CH, *Ar*), 128.2 (CH, *Ar*), 126.6 (CH, *Ar*), 125.4 (CH, *Ar*), 118.1 (CH, *Ar*), 88.9 (C, *Cp* ring), 83.1 (C, *Cp* ring), 69.5 (CH, *Cp* ring), 69.3 (CH, unsubstituted *Cp* ring), 65.8 (CH, *Cp* ring), 63.7 (CH, *Cp* ring), 50.1 (CH), 44.3 (CH₂), 13.1 (CH₃); IR (neat)/cm⁻¹ 3369 (*NH*), 2924, 2856, 1668, 1599, 1549, 1506, 1329, 1302, 1230, 1177, 1112, 851, 817; MS *m/z* (%) 506 (25) [*M*+*Na*]⁺, 484 (33) [*M*+*H*]⁺, 483 (100) [*M*]⁺, 303 (52) [*M*-*NHC(O)NHPhNO₂*]⁺; HRMS (ESI): *m/z* calcd for C₂₆H₂₅FeN₃O₃: 483.1240; found: 483.1237.

(*R*_p)-*N*-(4-Nitrophenyl)-*N*'-[2-methyl-ferrocenemethyl]-urea (*R*_p)-**3**. The amine (*R*_p)-**11** (183 mg, 0.80 mmol) was reacted with 4-nitrophenylisocyanate (164 mg, 1.00 mmol) and purified by flash column chromatography on silica gel (95:5 CH₂Cl₂/EtOAc, *R_f* = 0.7) to give the urea as a yellow powder (221 mg, yield 70%). Crystallographic quality crystals were obtained by slow evaporation of CH₂Cl₂ and Et₂O from a saturated solution at room temperature. *R_f* = 0.7 (CH₂Cl₂/EtOAc 95:5); m.p. 82–84°C; $[\alpha]_{\text{D}}^{25} = +75.3$ ($c = 0.74$ in chloroform); ¹H NMR (400 MHz, CD₂Cl₂) $\delta = 8.04$ (d, 2 H, $J = 9.2$ Hz, *ArH*),

7.45 (d, 2 H, $J = 9.2$ Hz, ArH), 6.89 (s, 1 H, ArNHC), 4.95 (t, 1 H, $J = 4.5$ Hz, CH₂NHC), 4.22 (dd, 1 H, $J = 14.2$ Hz, 5.7 Hz, CpCHHN), 4.11 – 4.01 (m, 3 H, CpH), 3.99 (s, 5 H, CpH), 3.92 (t, 1 H, *meta* H of Cp), 1.91 (s, 2 H, CpCH₃); ¹³C NMR (101 MHz, CD₂Cl₂) $\delta = 154.0$ (C, CO), 146.0 (C, Ar), 142.6 (C, Ar), 125.5 (CH, Ar), 118.1 (CH, Ar), 83.7 (C, Cp ring), 83.5 (C, Cp ring), 70.5 (CH, Cp ring), 69.6 (CH, unsubstituted Cp ring), 68.3 (CH, Cp ring), 66.4 (CH, Cp ring), 38.8 (CH₂), 13.1 (CH₃); IR (neat)/cm⁻¹ 3339, 3094, 2922, 1672, 1614, 1548, 1492, 1412, 1324, 1301, 1220, 1175, 1104, 1034, 998, 849, 747, 691; MS m/z [M+Na⁺]: 416.0; HRMS (ESI): m/z calcd for C₁₉H₁₉N₃O₃NaFe: 416.0674 [M+Na⁺]; found: 416.0679; elemental analysis calcd (%) for C₁₉H₁₉N₃O₃Fe·H₂O: C 57.51, H 4.93, N 10.59; found: C 57.51, H 4.86, N, 10.57; %ee = 97% by HPLC.

(S_p)-N-(4-Nitrophenyl)-N'-[2-methyl-ferrocenemethyl]-urea (S_p)-3. This was prepared as described above for (R_p)-3 using amine (S_p)-11 (160 mg, 0.70 mmol), giving the urea as brown yellow flakes (206 mg, yield 75%). Crystallographic quality crystals were obtained by slow evaporation of CH₂Cl₂ and Et₂O from a saturated solution at room temperature. $[\alpha]_D^{25} = -70.8$ ($c = 1.03$ in chloroform); elemental analysis calcd (%) for C₁₉H₁₉N₃O₃Fe: C 58.03, H 4.87, N 10.69; found: C 58.10, H 4.89, N 10.80; %ee = 91% by HPLC. Other characterisation data were in agreement with data for the other enantiomer (R_p)-3.

(R,R)-(-)-N,N'-[1-(1-Ferrocenyl-2-phenyl)-ethyl]-urea 5. The ferrocenyl amine **12^{6b}** (0.128 g, 0.42 mmol) was dissolved in DMF (2 mL) and added dropwise to a stirred mixture of 1,1'-carbonyldiimidazole (35 mg, 0.22 mmol) and DMF (5 mL). The mixture was stirred at room temperature overnight, then the crystallized solid imidazole was removed by filtration and the filtrate was concentrated *in vacuo*, dissolved in CH₂Cl₂, washed with water (3 x 10 mL), dried over anhydrous sodium sulphate, filtered and concentrated *in vacuo*. Purification by flash column chromatography (80% light petroleum, 20% EtOAc, R_f = 0.7) gave urea **5** as orange crystalline squares (74 mg, 56%). R_f = 0.77 (75% light petroleum, 25% EtOAc); m.p. 112–114 °C; $[\alpha]_D^{25} = -12.9$ ($c = 0.31$ in acetone); ¹H NMR (300 MHz, (CD₃)₂CO) $\delta = 7.26$ – 7.11 (m, 10 H, ArH), 4.93– 4.86 (m, 2 H, CH), 4.36– 4.34 (br, 2 H, NH), 4.14– 4.11 (m, 14 H, CpH), 4.03 (s, 2 H, CpH), 3.98 (s, 2 H, CpH), 3.09– 2.87 (m, 4 H, CH₂); ¹³C NMR (101 MHz, CD₃CN) $\delta = 157.6$ (quat. C, CO), 140.2 (quat. C, Ar), 130.4 (CH, Ar), 128.9 (CH, Ar), 126.9 (CH, Ar), 93.7 (quat. C, Cp), 69.4 (CH, Cp), 68.14 (CH, Cp), 68.08 (CH, Cp), 67.6 (CH, Cp), 66.8 (CH, Cp), 50.3 (CH, CpCHN), 43.7 (CH₂, CpCHCH₂); IR (neat)/cm⁻¹ 3357 (NH), 2972, 2921, 1630 (CO), 1549, 1495, 1454, 1410, 1319, 1248, 1106, 1078, 1048, 1027, 1001, 891, 819, 751; MS m/z (%) 675.1 (19) [M+K]⁺, 659.1 (74) [M+Na]⁺, 637.2 (100) [M+H]⁺, 289.1 (52) [CpFeCpCHCH₂Ph]⁺; HRMS (ESI): m/z calcd for C₃₇H₃₇Fe₂N₂O: 637.1599 [M+H]⁺; found: 637.1602; elemental analysis calc. (%) for C₃₇H₃₆Fe₂N₂O: C 69.8, H 5.7, N 4.4; found: C 69.6, H 5.8, N 4.15.

N,N'-Bis[1-ferrocenylmethyl]-urea 6. The ferrocenyl amine **13** (64 mg, 0.30 mmol) was dissolved in toluene (1 mL) and added dropwise to a stirred mixture of 1,1'-carbonyldiimidazole (24 mg, 0.15 mmol) and toluene (3 mL). The mixture was stirred at room temperature overnight, then the crystallized solid imidazole was removed by filtration and the filtrate was concentrated *in vacuo*, dissolved in CH₂Cl₂, washed with water (3 x 10 mL), dried over

anhydrous sodium sulphate, filtered and concentrated *in vacuo*.

The crude was purified by flash column chromatography (1:1 light petroleum/EtOAc) to yield the desired product as yellow crystalline needles (34 mg, 51%). Mp 232–236 °C; ¹H NMR (300 MHz, CD₂Cl₂) $\delta = 4.45$ (2 H, s, NH), 4.11 (4 H, s, H of substituted Cp ring), 4.08 (10 H, s, CpH), 4.04 (4 H, s, CpH), 3.97 (4 H, d, $J = 5.4$, CpCH₂); ¹³C NMR (101 MHz, CD₂Cl₂) $\delta = 157.5$ (C, CO), 86.6 (C, Cp ring), 68.9 (CH, Cp ring), 68.5 (CH, Cp ring), 68.4 (CH, Cp ring), 40.1 (CH₂); HRMS (ESI) m/z calcd for C₂₃H₂₄Fe₂N₂O₂Na: 479.0485 [M+Na⁺]; found: 479.0486. Elemental analysis calc. (%) for C₂₃H₂₄Fe₂N₂O: C, 60.56; H, 5.30; N, 6.14; found: C, 60.67; H, 5.36; N, 6.03.

(R_p)-1-(2-Methylferrocenyl)methanamine (R_p)-11. To a solution of (R_p)-2-methyl-ferrocenecarboxaldehyde (R_p)-10 (0.815 g, 3.60 mmol) in EtOH (5 mL) under argon was added a solution of hydroxylamine hydrochloride (4.39 mmol) in water (1.5 mL), followed by sodium acetate (6.57 mmol). The mixture was heated under reflux for 3 hours before the solvent was removed and CHCl₃ (6 mL) was added dropwise and the mixture stirred for an additional 30 minutes. The precipitated solid was filtered off and the filtrate was concentrated under vacuum to give the crude oxime as a brown-red oil. ¹H NMR (300 MHz, CDCl₃) $\delta = 8.12$ (1 H, s, CH=N), 4.56– 4.45 (1 H, m, *meta* H of Cp), 4.34– 4.23 (2 H, m, *ortho* H of Cp), 4.14 (5 H, m, unsubstituted Cp ring), 2.12 (3 H, s, CH₃). The oxime (0.685 g, 2.80 mmol) was then dissolved in dry THF (18 mL) and an excess of lithium aluminum hydride (0.49 g, 13 mmol) was carefully added and the mixture stirred under argon for 6 hours. Toluene (18 mL) was then added to the solution, followed by the careful addition of ethyl acetate (3.5 mL). A few drops of 5 M NaOH were then added until precipitation of inorganic species was complete. The mixture was filtered, yielding a yellow filtrate and a gummy solid residue. The residue was washed with copious amounts of toluene/MeOH (80:20). The filtrate was then evaporated to dryness and inorganic impurities removed by dissolution in dichloromethane followed by filtration and evaporation of the organic filtrate. The product was purified by flash column chromatography on silica, eluting with CH₂Cl₂ through to a mixture of 9:1 CH₂Cl₂/MeOH in the presence of a small amount of triethylamine, to yield the desired product as a brown yellow oil (0.272 g, yield 42%). ¹H NMR (300 MHz, CDCl₃) $\delta = 4.21$ (s, 1 H, *ortho* H of Cp), 4.09 (s, 2 H, *meta* H of Cp), 4.02 (s, 5 H, unsubstituted Cp ring), 3.67 (s, 2 H, CpCH₂N), 1.97 (s, 3 H, CpCH₃); ¹³C NMR (101 MHz, CDCl₃) $\delta = 88.7$ (C, Cp ring), 82.4 (C, Cp ring), 69.7 (CH, Cp ring), 68.9 (CH, unsubstituted Cp ring), 66.8 (CH, Cp ring), 65.3 (CH, Cp ring), 40.0 (CH₂, CpCH₂NH₂), 13.0 (CH₃, CpCH₃); MS m/z [M⁺-NH₂]: 213.0. HRMS (ESI): m/z calcd for C₁₂H₁₅NFe+Na⁺: 252.0452 [M+Na⁺]; found: 252.0450.

(S_p)-1-(2-Methylferrocenyl)methanamine (S_p)-11. The procedure described above was repeated to the same scale using (S_p)-2-methyl-ferrocenecarboxaldehyde (S_p)-10 (0.658 g, 2.89 mmol), giving the oxime as a brown-red oil (0.664 g, yield 95%). The oxime (0.664 g, 2.73 mmol) was then reduced with an excess of lithium aluminum hydride (0.45 g, 12 mmol) to yield the desired product as brown yellow oil (0.406 g, yield 65%) after column chromatography. Characterisation data were in agreement with data for the other enantiomer (R_p)-11.

Acknowledgements

We thank the EPSRC UK National Crystallography Service at the University of Southampton for the collection of the crystallographic data.

Notes and references

^a School of Chemistry, University of Birmingham, Edgbaston, Birmingham, B15 2TT, UK. Fax: +44 (0)121 414 4403; Tel: +44 (0)121 414 4422; E-mail: j.tucker@bham.ac.uk

^b School of Chemistry, University of Nottingham, University Park, Nottingham, NG7 2RD, UK.

† Electronic Supplementary Information (ESI) available: [Compound characterisation (NMR spectra), X Ray crystal structures, NMR Binding studies, UV/vis binding studies, electrochemistry including digital simulations]. See DOI: 10.1039/b000000x/CCDC 950562-950566.

- 1 L. Pu, *Acc. Chem. Res.*, 2012, **45**, 150-163.
- 2 For some reviews that cover aspects of electrochemical sensing using supramolecular receptors, see: (a) P. D. Beer, *Chem. Soc. Rev.*, 1989, **18**, 409-450; (b) P. L. Boulas, M. Gómez-Kaifer and L. Echegoyen, *Angew. Chem. Int. Ed.*, 1998, **37**, 216-247; (c) P. D. Beer, P. A. Gale and G. Z. Chen, *Adv. Phys. Org. Chem.*, 1998, **31**, 1.
- 3 For some relatively recent examples, see: (a) M. Alfonso, A. Tárraga and P. Molina, *Inorg. Chem.*, 2013, **52**, 7487-7496 and references therein; (b) N. H. Evans, C. J. Serpell, K. E. Christensen and P. D. Beer, *Eur. J. Inorg. Chem.*, 2012, 939-944; (c) A. Sola, A. Tárraga and P. Molina, *Dalton Trans.*, 2012, **41**, 8401-8409; (d) R. Pandey, R. K. Gupta, M. Shahid, B. Maiti, A. Misra and D. S. Pandey, *Inorg. Chem.* 2012, **51**, 298-311; (e) G. Gasser, C. Mari, M. Burkart, S. J. Green, J. Ribas, H. Stoeckli-Evans and J. H. R. Tucker, *New J. Chem.*, 2012, **36**, 1819-1827; (f) A. Lorenzo, E. Aller and P. Molina, *Tetrahedron*, 2009, **65**, 1397-1401. (g) S. Chowdhury, G. Schatte and H. B. Kraatz, *Eur. J. Inorg. Chem.* 2006, 988-993 (h) H. Miyaji, G. Gasser, S. J. Green, Y. Molard, S. M. Strawbridge and J. H. R. Tucker, *Chem. Commun.*, 2005, 5355-5357.
- 4 D. P. Cormode, A. J. Evans, J. J. Davis and P. D. Beer, *Dalton Trans.*, 2010, **39**, 6532-6541.
- 5 (a) A. Ori and S. Shinkai, *J. Chem. Soc., Chem. Commun.*, 1995, 1771 - 1772; (b) K. M. Chun, T. H. Kim, O. S. Lee, K. Hirose, T. D. Chung, D. S. Chung and H. Kim, *Anal. Chem.*, 2006, **78**, 7597-7600;
- 6 (a) P. Laurent, H. Miyaji, S. R. Collinson, I. Prokes, C. J. Moody, J. H. R. Tucker and A. M. Z. Slawin, *Org. Lett.*, 2002, **4**, 4037-4040; (b) Y. Willener, K. M. Joly, C. J. Moody and J. H. R. Tucker, *J. Org. Chem.*, 2008, **73**, 1225-1233.
- 7 G. Mirri, S. D. Bull, P. N. Horton, T. D. James, L. Male and J. H. R. Tucker, *J. Am. Chem. Soc.*, 2010, **132**, 8903-8905 and references therein.
- 8 K. M. Joly, C. Wilson, A. J. Blake, J. H. R. Tucker and C. J. Moody, *Chem. Commun.*, 2008, 5191-5193.
- 9 (a) C. J. Richards and A. J. Locke, *Tetrahedron-Asymmetry*, 1998, **9**, 2377-2407; (b) L. Schwink and P. Knochel, *Chem.-Eur. J.*, 1998, **4**, 950-968; T. J. Colacot, *Chem. Rev.*, 2003, **103**, 3101-3118.
- 10 O. Riant, O. Samuel, T. Flessner, S. Taudien and H. B. Kagan, *J. Org. Chem.*, 1997, **62**, 6733-6745.
- 11 V. I. Sokolov, L. L. Troitskaya and O. A. Reutov, *J. Organomet. Chem.*, 1979, **182**, 537-546.
- 12 H. Miyaji, S. R. Collinson, I. Prokes and J. H. R. Tucker, *Chem. Commun.*, 2003, 64-65.
- 13 H. B. Kraatz, *J. Organomet. Chem.*, 1999, **579**, 222-226.
- 14 S. Huikai, W. Qingmin, H. Runqiu, L. Heng and L. Yonghong, *J. Organomet. Chem.*, 2002, **655**, 182-185.
- 15 P. D. Beer and D. K. Smith, *J. Chem. Soc.-Dalton Trans.*, 1998, 417-423.
- 16 S. P. Rannard, N. J. Davis and I. Herbert, *Macromolecules*, 2004, **37**, 9418-9430.
- 17 (a) M. J. Hynes, *J. Chem. Soc.-Dalton Trans.*, 1993, 311-312; (b) Y. Molard, D. M. Bassani, J. P. Desvergne, N. Moran and J. H. R. Tucker, *J. Org. Chem.*, 2006, **71**, 8523-8531.
- 18 H. A. Benesi and J. H. Hildebrand, *J. Am. Chem. Soc.*, 1949, **71**, 2703-2707.
- 19 (a) M. Silva, A. J. L. Pombeiro, J. Dasilva, R. Herrmann, N. Deus, T. J. Castilho and M. Silva, *J. Organomet. Chem.*, 1991, **421**, 75-90; (b) M. Emilia, N. Silva, A. J. L. Pombeiro, J. Dasilva, R. Herrmann, N. Deus and R. E. Bozak, *J. Organomet. Chem.*, 1994, **480**, 81-90.
- 20 A. J. Bard and L. R. Faulkner, *Electrochemical Methods, Fundamentals and Applications*, Wiley, 2001.
- 21 J. E. B. Randles, *Trans. Faraday Soc.*, 1948, **44**, 327-338; A. Sevcik, *Collect. Czech. Chem. Commun.*, 1948, **13**, 349-377.
- 22 G. Ferguson, C. Glidewell, G. Opromolla, C. M. Zakaria and P. Zanello, *J. Organomet. Chem.*, 1996, **517**, 183-190.
- 23 (a) S. R. Miller, D. A. Gustowski, Z. H. Chen, G. W. Gokel, L. Echegoyen and A. E. Kaifer, *Anal. Chem.*, 1988, **60**, 2021-2024 (b) V. Amendola, L. Fabbrizzi and L. Mosca, *Chem. Soc. Rev.*, 2010, **39**, 3889-3915
- 24 D. D. Perin and W. L. F. Armarego, *Purification of Laboratory Chemicals*, Oxford, 1989.
- 25 P. A. Gale and S. J. Coles, *Chem. Sci.*, 2012, **3**, 683-689.
- 26 R. W. W. Hoof, 1998, *COLLECT Data Collection Software*, Nonius B. V., Delft.
- 27 Z. Otwinowski and W. Minor, in *Methods in Enzymology*, ed. C. W. Carter and R. M. Sweet, Academic Press, New York, 1997, vol. 276, pp. 307-326.
- 28 G. M. Sheldrick, 2007, *SADABS*, Bruker AXS Inc., Madison, Wisconsin, USA.
- 29 G. M. Sheldrick, *Acta Cryst.*, 2008, **A64**, 112-122.
- 30 L. J. Farrugia, *J. Appl. Cryst.*, 1997, **30**, 565.

Ferrocenyl urea receptors containing planar and central chirality electrochemically sense carboxylate anions via formation of H-bonded complexes

